Colloid Polym Sci (2008) 286:51–57
DOI 10.1007/s00396-007-1684-y

ORIGINAL CONTRIBUTION

Photoinduced redox reactions between colloidal manganese dioxide and some organic compounds of environmental importance

Ottó Horváth · Gergő Z. Bakota · Judit Marosfi · Zoltán Zsilák

Received: 9 February 2007 / Accepted: 25 March 2007 / Published online: 7 June 2007
© Springer-Verlag 2007

Abstract Numerous organic compounds of environmental importance, i.e., phenol, citric, tartaric, and oxalic acids, proved to promote or accelerate reductive dissolution of colloidal manganese dioxide upon irradiation. This is accounted for the formation of surface-located charge-transfer complexes between the MnO_2 particulates and the organic electron donors. From the dependences of the rate of the photoassisted and thermal dissolution on the concentration of the organic compounds, the equilibrium constants for the formation of these complexes have been determined in the case of phenol, resorcinol, citrate, and tartaric acid. The quantum yields for these photoinduced reactions (at λ_{ir}= 365 nm), however, do not show any correlation with the values of the corresponding equilibrium constants, although adsorption is prerequisite for the efficient reductive dissolution of MnO_2. The changes in pH markedly affect the rate of this process, indicating that protonation of both the electron donors and the surface of the MnO_2 particulates may play significant roles in these systems. The results of experiments carried out in manganese dioxide excess suggest that total mineralization of organic electron donors is strongly hindered by the disadvantageous adsorption properties of the primary redox products.

Keywords Photoredox · Manganese dioxide · Dissolution · Organic compounds · Surface complex

Dedicated to Professor Janos H. Fendler on the occasion of his 70th birthday.

O. Horváth (✉) · G. Z. Bakota · J. Marosfi · Z. Zsilák
Department of General and Inorganic Chemistry,
University of Pannonia,
8201 Veszprém P.O. Box 158, Hungary
e-mail: otto@vegic.uni-pannon.hu

Introduction

Manganese is the 11th most abundant element in the Earth's crust, and it is of considerable importance in natural aquatic systems [1, 2]. In natural waters, it occurs as insoluble Mn (III and IV) oxides and as soluble Mn^{2+} ions [3]. In oxygenated solutions, manganese (III, IV) oxide minerals are thermodynamically stable, and their formation in surface waters is a result of bacterial activity [4–7]. However, particulate Mn(IV) in aqueous systems can be reduced by organic compounds with carboxyl, carbonyl, phenolic, and alcoholic groups, enhancing the mobility of manganese [8–13]. At the same time, such reactions may contribute to the oxidative degradation of these organic electron donors occurring in natural waters even as pollutants [14–16].

Reactions between colloidal manganese dioxide and organic reductants, which play a key role in the redox cycling of manganese in the environment [17], can be accelerated or, moreover, initiated by photoexcitation [18, 19]. In these cases, irradiation in the visible and near ultraviolet range promotes the reductive dissolution of MnO_2, accompanied by the oxidation of organic pollutants in the system. Thus, sunlight can significantly influence the redox reactions of colloidal manganese dioxide in natural aquatic surface waters, affecting the biogeochemical cycle of manganese [6, 20–23]. Such electron transfer processes may decrease the concentrations of organic pollutants too. The aim of our study was to investigate the possibility and to elucidate the mechanism of the photoinduced charge-transfer reactions between colloidal MnO_2 and different organic electron donors of environmental importance. Utilizing these processes, the chance of mineralization of organic contaminants was also examined.

Experimental sections

Reagents and solutions Analytical grade $KMnO_4$, $MnSO_4 \cdot 4H_2O$, sodium polyphosphate ($(NaPO_3)_6$), benzoic acid, sodium benzoate, citric acid, sodium citrate, ethylenediaminetetraacetic acid (EDTA), sodium formate, maleic acid, malonic acid, oxalic acid, sodium oxalate, phenol, sodium phenolate, resorcinol, salicylic acid, sodium salicylate, tartaric acid, and sodium tartarate were used for the preparation of solutions studied. Triply distilled water served as the solvent. For dissolution experiments, a stock solution of 4×10^{-4} M MnO_2 was prepared by the synproportional reaction of MnO_4^- and Mn^{2+} according to a modified version of the process described in the literature [24]. A 75-cm^3 volume of 4×10^{-4} M $MnSO_4$ solution was added to 50 cm^3 of 4×10^{-4} M $KMnO_4$. To prevent precipitation of MnO_2 sodium polyphosphate was added to the $MnSO_4$ solution in the concentration of 4×10^{-4} M. This compound, as a polyelectrolyte, stabilized the produced colloid, so it did not change for weeks. In this case, however, the synproportional reaction is considerably slowed down because negatively charged polyphosphate repels MnO_4^- and bonds Mn^{2+}. Thus, the complete conversion takes several days. Nevertheless, this method ensures a good reproducibility (regarding the size distribution of the manganese dioxide particles) as it was proved by the same absorption spectra. It is worth mentioning, however, that excess of Mn^{2+} ions in this system significantly affects the absorption spectrum of the colloidal manganese dioxide. The position of the lower-energy band (at 370 nm) is shifted toward a longer wavelength, and the molar absorbances are considerably decreased upon increasing Mn^{2+} concentration. This observation indicates that Mn^{2+} ions are bound to the surface of the MnO_2 particles. Thus, deviating from our previous study [19], no Mn^{2+} excess was applied in the experiments of the present work during the preparation of colloidal MnO_2. For mineralization experiments, a stock solution of 1.2×10^{-2} M MnO_2 was prepared by an analogous method described above. Stock solutions were diluted to the concentrations applied for irradiation and kinetic measurements. If necessary, the pH was adjusted with NaOH and H_2SO_4 and measured with a SENTRON pH meter, using a glass electrode.

Photolysis For the study of photoinduced dissolution of colloidal MnO_2, the irradiations were carried out with 2.5-cm^3 solutions in 1-cm cells at room temperature. During the kinetic experiments, solutions were homogenized by magnetic stirring. For continuous photolysis at 365 nm, an AMKO LTI system consisting of a 150-W high pressure Xe–Hg arc lamp and a monochromator was applied. Incident light intensity was determined with a thermopile calibrated by ferrioxalate actinometry. Quantum yield measurements were carried out with samples of nearly 100% light absorption. For mineralization measurements, the irradiations were carried out at 20 °C in a glass-jacketed reactor vessel filled with 60 cm^3 of reaction mixture and wrapped with aluminum foil. A 125-W medium-pressure mercury lamp was applied as a radiation source. Mixing was accomplished by continuous bubbling of air through the solution.

Analysis The absorption spectra were recorded on a Specord S 100 diode array spectrophotometer, using 1-cm quartz cuvettes. Mineralization was followed by measuring the total organic carbon (TOC) concentration, utilizing a Thermo Electron Corporation TOC TN 1200 apparatus.

Results and discussion

Spectra, equilibrium, and reaction rate

In accordance with the earlier observations [19], the UV-vis absorption spectrum of the colloidal MnO_2 prepared in the way described in "Experimental sections" shows two broad overlapping bands with maxima at 215 and 370 nm (Fig. 1, curve a). In the concentration range examined (0–4×10^{-4} M), the Beer–Lambert's law is prevalid in this system, and for the peak of 370 nm, 9,330±90 M^{-1} cm^{-1} was obtained as molar absorbance. In agreement with our earlier study [19], the addition of phenol to colloidal manganese dioxide significantly changed the absorption band at 370 nm (Fig. 1, curve b). The band was shifted toward longer wavelengths in both works. In the previous study, however, its molar absorbance increased, while in the present case, its decreasing could be observed. This deviation is a consequence of the relatively high (20%) Mn^{2+} excess considerably diminishing the molar absorbance of the colloidal MnO_2. The spectral changes in both

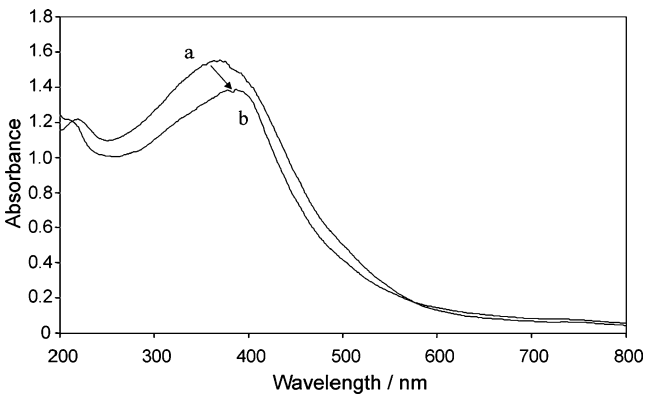

Fig. 1 Absorption spectrum of manganese dioxide (1.6×10^{-4} M) in the absence (**a**) and in the presence (**b**) of phenol (1×10^{-4} M; l=1 cm)

studies can be attributed to the formation of a surface complex (MnO_2–PhOH) as described by Eq. 1.

$$MnO_2(F) + PhOH \Leftrightarrow MnO_2 - PhOH = MnO_2(C) \quad (1)$$

"F" and "C" in parentheses designate free and complexed metal centers, respectively, on the surface of the MnO_2 particulates. The equilibrium constant of the above reaction is

$$K = \frac{[MnO_2(C)]}{[PhOH][MnO_2(F)]} \quad (2)$$

Because the molar absorbance of MnO_2(C) at the longer-wavelength (370–385 nm) band is lower than that of MnO_2(F) prepared in the present work (no Mn^{2+} excess) but higher than that in our previous study applying 20% Mn^{2+} excess, the directions of the change in the absorbance are opposite as indicated above.

On the basis of the observations with phenol, one could expect similar effects in the case of other organic electron donors as potential ligands. However, none of the numerous organic compounds we examined in this work displayed such an influence. Nevertheless, several of them strongly promoted the photoassisted reductive dissolution of colloidal MnO_2. In these cases, the dependence of the rate of the photochemical and/or thermal reactions on the concentration of the organic electron donor can be utilized for the estimation of the equilibrium constant (K) as it was proved for the instances of different colloidal metal oxides [19, 25–30]. The equilibrium constants calculated from the spectral changes and the reaction rates well agreed. In the latter method, the initial slope of the concentration vs irradiation time plot was taken as the rate of the disappearance (redox dissolution) of MnO_2. Concentrations were calculated from the absorbances measured at 370–385 nm, knowing the actual molar absorbances. When the rate of the photochemical reaction was determined, the overall rate of the MnO_2 dissolution was reduced by the thermal rate of reaction measured in the solution of the same composition (in the dark).

The rate of the redox dissolution of colloidal manganese dioxide in these systems is linearly proportional to the concentration of the surface-located charge-transfer complex formed between MnO_2 and the organic electron donor:

$$dC/dt \sim [MnO_2(C)]. \quad (3)$$

The concentration of the complexed MnO_2 can be expressed as the product of the total concentration of the colloidal manganese dioxide (C_{MnO2}) and the partial molar ratio of MnO_2(C) (α_C):

$$[MnO_2(C)] = \alpha_C C_{MnO2} \quad (4)$$

$$\alpha_C = K[D]/(1 + K[D]) \quad (5)$$

where D designates the organic electron donor.

Accordingly, the reaction rate vs α_C plot should also be linear. Using this correlation, the equilibrium constant (K) can be determined; during the procedure, we search for the value of K giving the best fit of this linear regression. This method, which is practically based on the Langmuir–Hinshelwood equation, can be used for both thermal and photoinduced reductive dissolution of colloidal manganese dioxide.

Selection of organic electron donors

The series of organic compounds we have tested are of mostly environmental importance, either as man-made pollutions or naturally produced materials, which may influence the biogeochemical cycle of manganese. For the test, the following compounds were chosen as candidates: benzoic acid, sodium benzoate, citric acid, sodium citrate, EDTA, sodium formate, maleic acid, malonic acid, oxalic acid, sodium oxalate, phenol, sodium phenolate, resorcinol, salicylic acid, sodium salicylate, tartaric acid, and sodium tartarate. Although our main purpose was to study the photoinduced charge transfer processes between them and colloidal manganese dioxide, thermal redox reactions taking place simultaneously in these systems could not be neglected either. Thus, before carrying out a systematic investigation of the light induced dissolution of MnO_2, preliminary experiments were done to select the electron donors (from the series of compounds above) in the case of which the photoassisted reaction is reasonably efficient. Thus, several of the original candidates had to be abandoned.

Practically, no permanent chemical change took place between colloidal MnO_2 and sodium benzoate, neither in the dark nor upon irradiation. Only thermal redox reactions were observed with EDTA, malonic acid, sodium formate, and sodium phenolate. Benzoic acid, maleic acid, and sodium tartarate displayed only negligible photochemical reaction. On the contrary, in the case of salicylic acid and sodium salicylate, in the applied concentration range (10^{-5}–10^{-3} M), the thermal reactions were too fast to follow the changes by a steady-state spectrophotometric method and to separate the photoinduced dissolution upon irradiation. Thus, there remained seven candidates for systematic investigation.

Comparison of photoinduced and thermal dissolution of colloidal MnO_2 for various electron donors

To compare the effect of the photoinduced processes with that of the thermal dissolution, experiments were carried out both in the dark and under irradiation. The concentration of the electron donor was 10^{-3} M for all candidates previously selected. The data of Table 1 summarizes the initial rates of the overall reductive dissolution (measured under irradiation), those of the thermal reaction (determined under the

Table 1 Dissolution rates of MnO_2 (1.6×10^{-4} M) in the presence of various organic electron donors (1.0×10^{-3} M)

Organic electron donor	Overall (10^{-5} M min^{-1})	Thermal (10^{-5} M min^{-1})	Photoinduced (10^{-5} M min^{-1})
sodium oxalate	0.485	0.088	0.398
oxalic acid	13.30	8.29	4.97
sodium citrate	0.375	0.000	0.375
citric acid	3.71	0.408	3.30
tartaric acid	0.824	0.370	0.454
resorcinol	2.81	1.75	1.06
phenol	2.36	1.31	1.05

same circumstances but in the dark), and their difference as the rate of the photochemical process.

These data indicate that in the case of oxalate, the rate of the thermal reaction is about one fifth of that of the photoinduced process. The photoassisted reaction of oxalic acid is one order of magnitude faster than that of oxalate but the rate of its thermal reaction is significantly higher. For citric acid, the thermal reaction is about one order of magnitude slower than the photochemical process. In addition, for the corresponding salt (sodium citrate), similarly to the oxalic acid–oxalate pair, the photoinduced (and also the overall) dissolution rate is one order of magnitude lower than that for the acid. Notably, from the organic electron donors, this is the only case where no thermal reaction can be observed. For resorcinol, phenol, and tartaric acid, the rates of photoassisted and thermal processes are comparable. Because the photochemical dissolution in the system containing sodium tartarate was negligible (see "Selection of organic electron donors"), our observations on the three acid–anion pairs suggest that the protonated (acid) forms more (one order of magnitude higher) effectively promote the reductive dissolution of MnO_2 than the corresponding (deprotonated) anions. This phenomenon can be attributed to either the different adsorptions on the surface of the manganese dioxide particles or the pH dependence of the redox reactions taking place in the dissolution process.

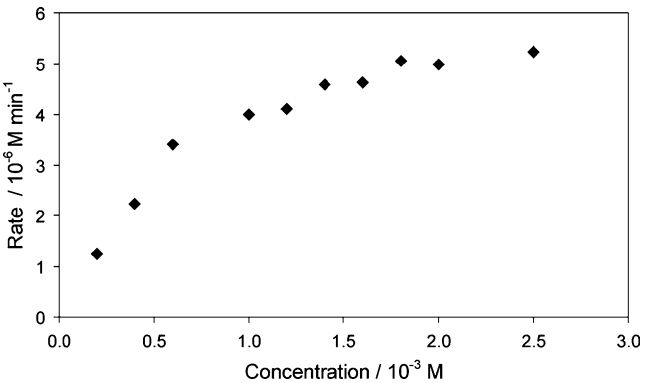

Fig. 2 Photochemical dissolution rate of MnO_2 (1.6×10^{-4} M) as a function of the concentration of added tartaric acid

Dissolution rates, equilibrium constants, and quantum yields

In the cases of resorcinol, phenol, citrate, and tartaric acid, increasing the concentration of organic electron donor added, the dissolution rate is linearly increased in the initial part of the concentration range studied, then the slope of the rate vs [D] function gradually decreases. This phenomenon is well demonstrated by Fig. 2 for tartaric acid. This Langmuir-type curve clearly shows that, in accordance with the earlier observations [18, 19], the dissolution rate linearly depends on the concentration of the charge-transfer complex formed on the surface of the colloidal manganese dioxide particles. The quantitative description of this correlation involves the partial molar ratio of the complexed MnO_2 (see Eqs. 3–5 in "Spectra, equilibrium, and reaction rate"). Hence, plotting the rates as a function of α_C, the equilibrium constant (K) can be obtained if the value of K giving the best fit of the linear regression is found. Theoretically, this linear function starts from the origin. In accordance with this theory, Fig. 3 unambiguously shows a linear fit on the corresponding data of the tartaric acid system. In this case, $K=1{,}400\pm100$ M^{-1} has been determined for the equilibrium constant from the data regarding the photoinduced dissolution. For resorcinol, the rates of both the thermal and the photoassisted reaction were utilized for the determination of K (Figs. 4 and 5). The

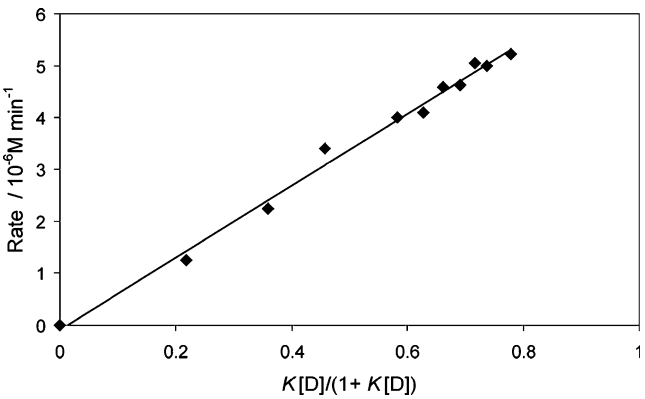

Fig. 3 Photochemical dissolution rate of MnO_2 (1.6×10^{-4} M) as a function of the partial molar ratio of the surface-localized charge-transfer complex (between MnO_2 and D = tartaric acid, $K=1{,}400$ M^{-1})

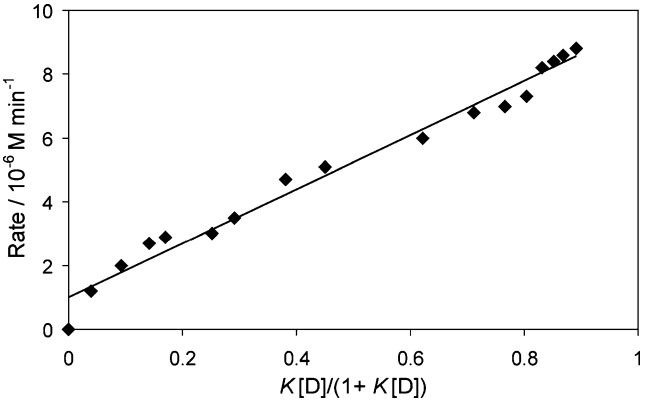

Fig. 4 Photochemical dissolution rate of MnO_2 (1.6×10^{-4} M) as a function of the partial molar ratio of the surface-localized charge-transfer complex (between MnO_2 and D = resorcinol, K=4,100 M^{-1})

values of K determined for the different electron donors studied are summarized in Table 2.

In the cases of citric acid, oxalic acid, and sodium oxalate, the initial dissolution rate vs [D] functions gave straight lines in the concentration range studied as demonstrated by Fig. 6. From these data, no equilibrium constant can be determined because the saturation part of the Langmuir-type function has not been reached yet. Therefore, only an estimation for the upper limit of the order of magnitude for K can be made. Thus, taking 2×10^{-3} M as maximum [D] and 10% measurement error, K cannot exceed 50 M^{-1}.

The efficiency of photoinduced reactions can be quantitatively characterized by the quantum yield. It gives the number of molecules or ions converted or formed as a result of absorption of one photon. Table 2 also contains the quantum yields determined for the photoinduced dissolution of MnO_2 in the presence of various electron donors (10^{-3} M) at 365-nm irradiation. Comparing these data with the corresponding equilibrium constants, it is clearly seen that there is no correlation between these parameters. This observation suggests that even relatively weak adsorption is enough for an effective photoinduced (or thermal) charge

Table 2 Equilibrium constants (K) for the complex formation between MnO_2 and different organic electron donors and quantum yields for the photoreductive dissolution of colloidal manganese dioxide (1.6×10^{-4} M) in the presence of these reductants

Organic electron donor	Complex formation constant (M^{-1}; thermal)	Quantum yield (λ_{ir}= 365 nm, $C_D=10^{-3}$ M)
sodium oxalate	<50	3.4×10^{-5}
oxalic acid	<50	1.64×10^{-3}
sodium citrate	1,500	1.51×10^{-5}
citric acid	<50	8.1×10^{-5}
tartaric acid	1,400 (2,600)	7.8×10^{-5}
resorcinol	4,100 (4,900)	3.1×10^{-4}
phenol	18,300 (20,100)	3.2×10^{-4}

transfer reaction, or, reversely, a rather strong adsorption (or formation of a surface complex) does not necessarily ensure high efficiency for the reductive dissolution.

Nevertheless, the general mechanism for the reductive dissolution of a metal (hydr)oxide such as MnO_2 includes the following steps [18, 31–33]: (1) surface complex formation between the adsorbed ligand and the surface metal center, (2) electron transfer within the surface-located complex, giving a reduced surface metal center and the oxidized ligand, and (3) detachment of the reduced surface metal center.

Effects of pH on the dissolution rate

Because in the previous experiments no added acid or base was applied for pH adjustment, the values of pH in the systems studied were determined by the protonation and dissociation of the reactants, the colloidal manganese dioxide and the actual electron donor. To elucidate the effects of pH on the reductive dissolution of MnO_2, however, systematic change of the pH value was necessary in the case of selected electron donors. For this purpose, citric acid and tartaric acid

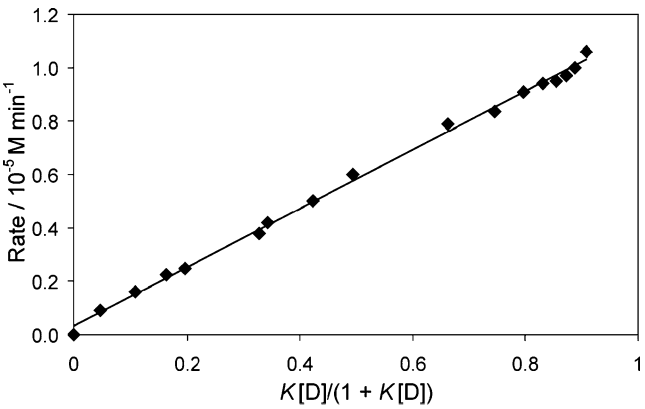

Fig. 5 Thermal dissolution rate of MnO_2 (1.6×10^{-4} M) as a function of the partial molar ratio of the surface-localized charge-transfer complex (between MnO_2 and D = resorcinol, K=4,900 M^{-1})

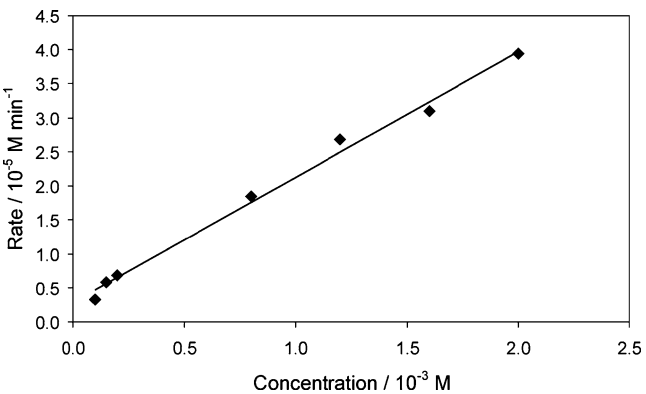

Fig. 6 Photochemical dissolution rate of MnO_2 (1.6×10^{-4} M) as a function of the concentration of added citric acid

were chosen as electron donors, and the value of pH was changed in the ranges of 3–10 and 3–12, respectively.

As Figs. 7 and 8 indicate, the rate of dissolution is significantly higher at lower values of pH than in basic systems. This observation is in accordance with the role of H^+ in the redox reactions taking place in the dissolution as exampled by Eq. 6 where citric acid is the electron donor.

$$9\ MnO_2 + C_6H_8O_7 + 18\ H^+ \rightarrow 6\ CO_2 + 9\ Mn^{2+} + 13\ H_2O \quad (6)$$

From this overall stoichiometric equation, the order of the pH effect cannot be predicted because it depends on the rates of the elementary steps in the mechanism, which must be different for the various electron donors. Nevertheless, the formation of water-soluble Mn^{2+} ions is accompanied by the reaction (fixation) of the formal oxide ions deliberated from MnO_2, and this process is certainly promoted by H^+ ions.

Besides the overall stoichiometry of the redox reactions, protonation must also play an important role in these systems from the viewpoint of adsorption as the characteristics of the rate vs pH plots suggests. The correlations between the protonation constants for both tartaric acid ($lg\beta_1$=4.1, $lg\beta_2$=7.0) and citric acid ($lg\beta_1$=5.4) [34] and the breakpoints of the corresponding plots suggest that protonated forms owing to their neutralized or diminished negative charge can be adsorbed more easily on the surface of the colloidal manganese dioxide particles. Because the pH of zero point of charge for MnO_2 is in the range of 2–4 [35], in the systems with low values of pH, the release of Mn^{2+} ions formed in the redox process is promoted, increasing the accessibility of the unreacted Mn(IV) sites and thus the rate of the reductive dissolution.

Mineralization of citrate

While reductive dissolution of colloidal MnO_2 is mostly important from the viewpoint of the speciation and biogeochemical cycling of manganese in the nature, this process may also be worth studying from the side of the potential organic electron donors, which can occur in both surface waters and wastewaters. Therefore, the degradation of such organic compounds, accompanying the dissolution of manganese dioxide, may play a considerable role in the self-cleaning of natural waters, and it might be utilized in the treatments of various wastewaters. Thus, we also carried out experiments focusing on the oxidative degradation, possibly mineralization, of the organic electron donor. In the case of mineralization, the organic contaminant is converted to simple inorganic compounds such as water and carbon dioxide. For the study of the degradation of the electron donor, deviating from the previous experiments regarding the dissolution of MnO_2, manganese dioxide was applied in significant excess so that its consumption does not influence the rate of the mineralization. Thus, the concentration of the colloidal MnO_2 was 5×10^{-3} M, while that of the electron donor was 2.5×10^{-4} M. For these model experiments, sodium citrate was chosen as the organic compound to be degraded because its photoinduced reaction with manganese dioxide displayed an acceptable rate, and no thermal dissolution was observed in the presence of this electron donor (see Table 1). The

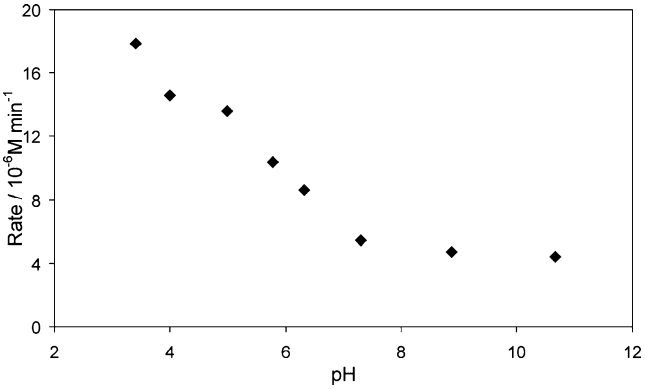

Fig. 8 Photochemical dissolution rate of MnO_2 (1.6×10^{-4} M) in the presence of 10^{-3} M tartaric acid as a function of pH

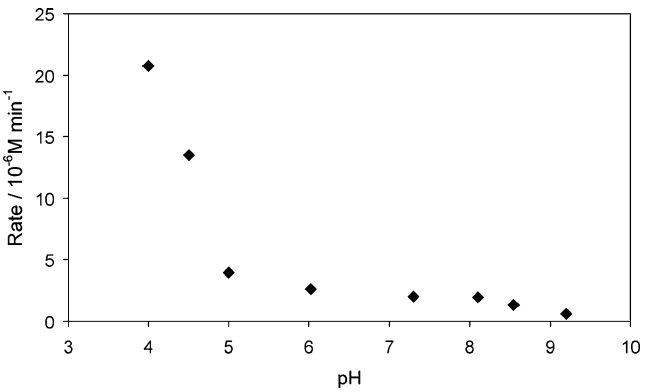

Fig. 7 Photochemical dissolution rate of MnO_2 (1.6×10^{-4} M) in the presence of 10^{-3} M citric acid as a function of pH

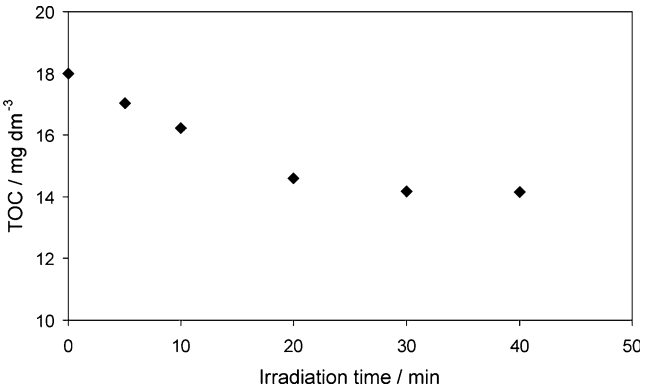

Fig. 9 Change of total organic carbon concentration (*TOC*) as a function of time during the irradiation of solution containing 5.0×10^{-3} M MnO_2 and 2.5×10^{-4} M sodium citrate

mineralization of citrate was followed by measuring the TOC concentration in the system irradiated.

As the experimental data indicate (Fig. 9), in the first 20-min period of the photolysis, the decrease of the TOC, i.e., the rate of the mineralization was rather significant, approx. 20% of the initial amount of citrate was converted to water and carbon dioxide (or carbonate). However, further irradiation did not cause any considerable change in the value of TOC. This phenomenon may be attributed to at least two effects. On the one hand, the inner Mn(IV) sites of the colloidal manganese dioxide particles are not accessible for the reducing reactants (for either the initial citrate ions or the intermediates formed in their oxidation) maybe because of the blocking effect of the Mn(III) and Mn(II) species formed on the surface because of a rather slow desorption. On the other hand, the intermediate oxidation products are not adsorbed on the surface of the MnO_2 particle as strongly as citrate ions are. Both effects may be influenced by protonation and deprotonation of the interacting species. Thus, further experiments at different values of pH ought to be carried out with this system to unambiguously elucidate the mechanism of mineralization and to improve its efficiency.

Conclusion

Various organic compounds of environmental importance promote or accelerate reductive dissolution of colloidal manganese dioxide upon irradiation. This phenomenon is attributed to the formation of surface-located charge-transfer complexes between the MnO_2 particulates and the organic electron donors. The equilibrium constants for the formation of these complexes were determined from the dependences of the rate of the photoassisted and thermal dissolution on the concentration of the organic compounds in the case of phenol, resorcinol, citrate, and tartaric acid. Although adsorption is prerequisite for the efficient reductive dissolution of MnO_2, the quantum yields for these photoinduced reactions (at λ_{ir}=365 nm) do not show any direct correlation with the corresponding equilibrium constants. The effects of pH on the rate of this process indicate that protonation of both the electron donors and the surface of the MnO_2 particulates may play considerable roles in these systems. Partial mineralization of citrate achieved in manganese dioxide excess suggests that total conversion of organic electron donors to inorganic compounds is strongly hindered by the disadvantageous adsorption properties of the primary redox products. Unambiguous elucidation of this phenomenon needs further investigation.

Acknowledgment This work was supported by the Industrial Foundation for the Engineers' Training in Veszprém. OH is especially grateful to Professor Janos H. Fendler for the invaluable help, in both professional and private respects, giving considerable guidance in the modern colloid chemistry and inspiration for the research in this field.

References

1. Papp S, Kümmel R (1988) Umweltchemie. Deutscher Verlag für Grundstoffchemie, Leipzig
2. Glasby GP (1984) Oceanogr Mar Biol Annu Rev 22:169
3. Stumm W, Morgan JJ (1981) Aquatic chemistry: an introduction emphasizing chemical equilibria in natural waters. Wiley, New York
4. Tebo BM, Nealson KH, Emerson S, Jacobs L (1984) Limnol Oceanogr 29:1247
5. Tebo BM, Emerson S (1985) Appl Environ Microbiol 50:1268
6. Sunda WG, Huntsman SA (1988) Deep-Sea Res 35:1297
7. Sunda WG, Huntsman SA (1990) Limnol Oceanogr 35:325
8. Sunda WG, Huntsman SA, Harvey GR (1983) Nature 234:301
9. Stone AT, Morgan JJ (1984) Environ Sci Technol 18:450
10. Khan Z, Kumar P, Kabir-ud-Din (2004) Colloids Surf A Physicochem Eng Asp 248:25
11. Andrabi SMZ, Khan Z (2005) Colloid Polym Sci 284:36
12. Wang Y, Stone AT (2006) Geochim Cosmochim Acta 70:4463
13. Wang Y, Stone AT (2006) Geochim Cosmochim Acta 70:4477
14. Baker WE (1973) Geochim Cosmochim Acta 37:269
15. Guy RE, Chakrabarti CL (1976) Can J Chem 54:2600
16. Sunda WG, Kieber DJ (1994) Nature 367:62
17. Ulrich HJ, Stone AT (1989) Environ Sci Technol 23:421
18. Xyla AG, Sulzberger B, Luther GW III, Hering JG, Van Cappellen P, Stumm W (1992) Langmuir 8:95
19. Horváth O, Strohmayer K (1998) J Photochem Photobiol A Chem 116:69
20. Sunda WG, Huntsman SA (1983) Limnol Oceanogr 28:924
21. Waite TD, Szymczak R (1994) In: Helz GR, Zepp RG, Crosby DG (eds) Aquatic and surface photochemistry. Lewis, Boca Raton, p 39
22. Sunda WG, Huntsman SA (1994) Mar Chem 46:133
23. Matsunaga K, Ohyama T, Kuma K, Kudo I, Suzuki Y (1995) Water Res 29:757
24. Lume-Pereira C, Baral S, Henglein A, Janata E (1985) J Phys Chem 89:5572
25. Waite TD, Morel FMM (1984) J Colloid Interface Sci 1:102
26. Waite TD, Wrigley IC, Szymczak R (1988) Environ Sci Technol 22:778
27. Dzombak DA, Morel FMM (1990) Surface complexation modeling. Wiley, New York
28. Blesa MA, Morando PJ, Regazzoni AE (1994) Chemical dissolution of metal oxides. CRC, Boca Raton
29. Sulzberger B, Laubscher H, Karametaxas G (1994) In: Helz GR, Zepp RG, Crosby DG (eds) Aquatic and surface photochemistry. Lewis, Boca Raton, p 53
30. Rodenas LAG, Iglesias AM, Weisz AD, Morando PJ, Blesa MA (1997) Inorg Chem 36:6423
31. Sulzberger B, Suter D, Siffert C, Banwart S, Stumm W (1989) Mar Chem 28:127
32. Stumm W, Sulzberger B, Sinniger J (1990) Croat Chem Acta 63:277
33. Borer PM, Sulzberger B, Reichard P, Kraemer SM (2005) Mar Chem 93:179
34. Perrin DD (1979) IUPAC Chemical Data Series—no. 22: stability constants of metal–ion complexes, part B: organic ligands. Pergamon, Oxford
35. McKenzie RM (1981) Aust J Soil Res 19:41